Polymer Chemistry

ROYAL SOCIETY OF CHEMISTRY

PAPER

View Article Online
View Journal | View Issue

Cite this: *Polym. Chem.*, 2025, **16**, 2401

Alkali lignin stabilization of oil-in-water emulsions *via* simple dispersion and ozonation processes†

Maëva Peloille,[a] Frédérique Ham-Pichavant,[a] Marie Reulier,[b] Cécile Joseph,[b] Henri Cramail *[a] and Stéphane Grelier *[a]

An alkali lignin was subjected to successive processes enabling the stabilization of oil-in-water (O/W) emulsions. Firstly, by merely using a water/acetone mixture and evaporating acetone, more than 90% of this lignin could be dispersed in pure water, with no chemical modification involved. The obtained lignin dispersion was then subjected to an ozonation reaction, without requiring any additional steps, resulting in an increase of the carboxylic acid content (+193%), through effective cleavage of phenolic structures (−93%), and a decrease in the lignin molar masses, as evidenced by ^{31}P quantitative NMR, 2D HSQC NMR, FT-IR spectroscopy and size-exclusion chromatography. These features allowed this alkali lignin to be easily re-dispersed in water. Aqueous dispersions of lignin before and after ozonation were characterized by an acidic pH and a bimodal nano-objects composition. These nano-objects exhibited a great affinity for interfaces, especially the ozonated lignin with an ability to reduce the surface tension of water down to 48 mN m^{-1} and the interfacial tension of a water/sunflower oil system down to 8 mN m^{-1}. Both lignins were consequently involved in the preparation of O/W emulsions and were able to stabilize micro-sized oil droplets, through a supposed Pickering mechanism, preventing oil release under both accelerated and real-time conditions (30 days). These results demonstrated that stable emulsions could be obtained from simply processed lignins for potential applications in cosmetic formulations or for the entrapment of hydrophobic compounds in the agrochemical or pharmaceutical industries.

Received 30th March 2025,
Accepted 19th April 2025

DOI: 10.1039/d5py00319a

rsc.li/polymers

Introduction

The rapid depletion of non-renewable resources has led academy and industry to turn towards biomass utilization for the production of more sustainable energy and chemical derivatives. Amongst the different sources of biomass, the lignocellulosic biomass, mostly composed of cellulose, hemicelluloses and lignin, is highly abundant, representing 181.5 billion tons annually, and does not compete with human food supplies.[1] Lignin accounts for 20 to 35% of lignocellulosic biomass, as it is one of the major components of terrestrial plant cell walls providing strength, cohesion, or resistance against pathogens, facilitating water transport and more.[2,3] Lignin is the primary source of aromatic structures in nature and is biosynthesized from phenylpropanoid units known as monolignols, which differ in the number of methoxy groups attached to their aromatic rings. Lignification is initiated by enzymatic oxidative dehydrogenation reactions, driven by the coupling of the resulting radicals, and leads to the formation of characteristic lignin structural patterns.[4]

The lignin structure depends on its botanical source as well as the extraction process used. The extraction of technical lignins is closely tied to the pulp and paper industries, which have developed various extraction technologies to separate cellulose from the other lignocellulose components. Approximately 70 million tons of lignin are extracted each year, yet only 2% are converted into high value-added products,[5] despite lignin's set of interesting properties such as antioxidant, anti-UV, or anti-microbial abilities.[6] Lignin contains hydrophilic segments (hydroxyl groups, sulfonate moieties in the case of lignosulfonates) as well as hydrophobic segments (aromatic rings) endowing it with amphiphilic properties and surface activity. Lignosulfonates, in particular, are commercialized as anionic flocculants, dispersants, or surfactants, applications that exploit their solubility in water and surface properties.[7] However, lignosulfonate may be too hydrophilic and/or not pure enough to effectively stabilize emulsions.[8] This can be improved by combining lignosulfonates

[a]*Université de Bordeaux, CNRS, Bordeaux INP, LCPO, UMR 5629, F-33600 Pessac, France. E-mail: sgrelier@enscbp.fr, henri.cramail@enscbp.fr*
[b]*ITERG, 11 rue Gaspard Monge, 33610 Canéjan, France*

†Electronic supplementary information (ESI) available: Provide additional experimental details including details about lignin characterization, ozonation reaction protocol, optimization and mechanism. Additional data about particles and oil droplet sizes, transmission profiles obtained from analytical centrifugation as well as some additional stability results illustrating the effect of pH. See DOI: https://doi.org/10.1039/d5py00319a

with co-surfactants for instance,[9] but other types of technical lignins also exhibit surface properties. Alkali, Kraft, Organosolv or enzymatic-hydrolyzed lignins are often submitted to chemical modification to modulate their amphiphilicity.[8] Hydrophilicity could be enhanced by attaching poly (ethylene glycol) (PEG) chains *via* grafting-on[10,11] or grafting-from[12] strategies. Gupta *et al.*[13] used a Kraft lignin as macro-initiator for the reversible addition–fragmentation chain-transfer (RAFT) polymerization of hydrophilic acrylic acid and acrylamide. Ionized or ionizable groups such as carboxylic acid groups have also been incorporated into lignin through carboxymethylation,[14,15] sulfoethylation,[16] Mannich reaction,[17,18] the latter enabling the introduction of lysine or quaternary ammonium groups, for instance. New carboxylic acids could also be introduced thanks to oxidation reactions,[19,20] while Gharehkhani *et al.*[21] successfully attached tannic carboxylic acids through oxidation, transesterification and ring-opening reactions. Zwitterionic lignin were obtained by successive oxidation, sulfonation and alkylation reactions[22] or through sulfonation followed by Mannich reactions.[23] Other approaches aimed at improving lignin hydrophobicity by subjecting it to alkylation,[24] or esterification[25,26] reactions, that could lead to water-in-oil (W/O) emulsions. Some studies describe combined strategies to add both hydrophobic and hydrophilic or ionized moieties.[27,28] The modified lignins generally display improved surface activities and emulsion stabilization abilities compared to the starting lignin. Finally, some unmodified technical lignins have also been involved in the preparation of O/W emulsions.[29–31] All these studies highlight the key roles of the molar masses, the nature and structures of chemical groups, the degree of substitution in modified lignins, the charge density, the purity, or the chemical stability of lignin in the emulsion stabilization mechanisms, which mainly involve electrostatic and steric effects at the interfaces. Such systems could find applications in cosmetic or detergent formulations,[19,32] phytosanitary agents encapsulation,[17] enhance oil recovery,[22,27] bitumen stabilization,[15,18] to name a few.

However, the large-scale production of lignin-based stabilization agents would require greener processes. The principles of green chemistry involve utilization of biomass like lignin but also emphasize waste prevention, the use of harmless solvents, or the design of efficient chemical reactions.[33] These principles must be taken into account in the manufacturing of more sustainable products. In this work, our first goal was to solubilize an alkali lignin in water through a simple two-step process using only water and acetone, both recognized as green solvents. Subsequently, we employed ozonation as a modification strategy to enhance lignin hydrophilicity under aqueous conditions. The resulting lignins were characterized in terms of particle size, morphologies and surface properties. Surface and interfacial tensions measurements were also conducted to assess the lignins' affinity for, and ability to adsorb at, both water/air and water/oil interfaces. These lignins were consequently involved in the formulation of oil-in-water (O/W) emulsions and compared to a commercial lignosulfonate in terms of emulsion stabilization through droplet size and behavior characterization or analytical centrifugation means.

Experimental section

Materials

Alkali lignin (AL) was extracted from *Pinus pinaster* and supplied by RYAM (Tartas, France). It was obtained *via* alkaline extraction from wood pulp processed through a bisulfite method using HSO_3^- and NH_4^+ at 150 °C, 8–9 bars, for 6–8 hours. The extraction was carried out under heating, followed by precipitation under acidic conditions. A lignosulfonate (LS) extracted according to the same bisulfite process was also provided by RYAM. Acetone (technical grade), and deuterated dimethyl sulfoxide (DMSO-d_6, 99.8%D) were purchased from VWR. Deuterated chloroform ($CDCl_3$, 99.5%D) was purchased from Eurisotop. Sodium hydroxide (NaOH, 98%) and pyridine (≥99%) were purchased from Fisher Scientific. Potassium iodide (KI, 99%), dimethylformamide (DMF, 99.5%), 2-chloro-4,4,5,5-tetramethyl-1,3,2-dioxaphospholane (TMDP, 95%), *endo-N*-hydroxy-5-norbornene-2,3-dicarboximide (HONB, 97%), and chromium(III) acetylacetonate ($Cr(acac)_3$, 99.99%) were purchased from Sigma-Aldrich. Oxygen (O_2, 99.9995%) was obtained from MESSER, and sunflower oil was sourced from a local supermarket. Pyridine, DMF, and $CDCl_3$ were dried prior to use, while the other chemicals were used without further purification.

Solubilization of AL in water

In the first step, AL (5, 10 or 20 g) was slowly added to a 50 : 50 (v/v) mixture of acetone and Milli-Q water at a concentration of 10 wt%. The brown mixture was stirred magnetically at 400 rpm for 2 hours at room temperature. After two hours, the mixture was centrifuged at 4550*g*, at 4 °C for 25 minutes. The pellet was vacuum-dried in an oven to determine the mass balance. The supernatant was collected, and the acetone in the mixture was evaporated using a rotary evaporator. After the complete evaporation of acetone, water was added to the mixture to maintain a concentration of 10 wt%. The second step was carried out under the same conditions as the first: 2 h, room temperature, 400 rpm stirring. After two hours, the mixture was centrifuged again (4550*g*, 4 °C, 25 min) to separate the pellet, which was dried for mass balance determination, and the supernatant, which was kept in its current state (Hydr-AL). A sample of the supernatant was freeze-dried for characterization purposes. Dilutions, when necessary, were conducted with Milli-Q water. All lignin aqueous solution were stored at 4 °C, protected from light.

Lignin ozonation

The previously obtained aqueous solution of lignin (2 mL) was diluted tenfold and introduced into a glass chemical reactor equipped with several inlets and outlets. One inlet was connected to a *corona* ozone generator (C-L010-DS, Airtree Ozone Technology Co.), which was further linked to a pure oxygen

bottle. An outlet was connected to a KI trap used to decompose the residual ozone (Fig. S1†). The power of the electric field producing ozone was set to the maximum value while the gas flow was kept to 5 L min^{-1}. Ozone produced by the generator was directly bubbled into the lignin solution, with constant stirring, at room temperature for 10 minutes. At the end of the reaction, the mixture was allowed to rest to remove the foam formed by the gas bubbling and was then freeze-dried and weighted. Knowing the initial lignin concentration, it was possible to determine the product mass yield (Ozon-AL). For the solubility tests, the ozonated lignin was introduced in Milli-Q water at a concentration of 2.5 wt%. The mixture was centrifuged (5000*g*, 25 °C, 10 min) and both the supernatant and pellet were dried before being weighted.

Lignin characterization

Quantitative ^{31}P NMR was employed to quantify lignin hydroxyl groups, following a procedure extensively detailed in previous studies,[34] which involves lignin derivatization. Briefly, 30–35 mg of dried lignin sample, 3–5 mg of internal standard HONB and 1 mg of relaxation agent $Cr(acac)_3$ were precisely weighted and solubilized in 500 μL of anhydrous pyridine/$CDCl_3$ (1.6 : 1 v/v) mixture under inert atmosphere. To aid solubilization, 500 μL of DMF were added. Then 50 μL of derivatization agent TMDP were added, and the reaction was allowed to complete 50 min at room temperature. Following the reaction, 400 μL of the mixture and 200 μL of $CDCl_3$ were introduced into a 5 mm borosilicate NMR tube. The acquisition was performed at 298 K on a Bruker Avance III spectrometer (400 MHz) with a relaxation time of 5 seconds and 256 scans. The spectra were calibrated using the internal standard signal (δ = 151.9 ppm) as a reference. The hydroxyl group content was determined by integrating the signals corresponding to specific chemical shifts: 149.5–145.5 ppm for the aliphatic OH (Aliph-OH), 144.5–137.4 ppm for the phenolic OH (Ph-OH), 136–134 ppm for the carboxylic acids (CO-OH) (Fig. S2†).

Heteronuclear Single Quantum Coherence (HSQC) 2D NMR was performed at 296 K on a Bruker Avance NEO spectrometer (400 MHz) equipped with a BBO Prodigy cryo-probe. The pulse program was hsqcetgpsisp2.2. The spectra were acquired with 32 scans. Lignins (40 mg) were dissolved in 50 μL of DMSO-d_6. The central solvent peak was used as internal reference (DMSO 39.5/2.5 δ_C/δ_H). Signal attribution was made based on previous studies.[35]

Fourier transform infrared spectroscopy (FT-IR) analyses were performed thanks to a Bruker Vertex 70 apparatus in attenuated total reflectance (ATR) mode equipped with a GladiATR diamond. The spectra were recorded in the range of 4000 to 400 cm^{-1}, using 64 scans with a resolution of 4 cm^{-1}.

Molar masses were analyzed by size-exclusion chromatography (SEC) using a NaOH solution (pH 12) as the eluent. The analysis was performed on a three-column system (TSKgel G4000PW + G3000PW + G3000PW, Tosoh) equipped with a guard column (TSKgel PWH, Tosoh) at 26 °C, 38 bars, and a flow rate of 1.0 mL min^{-1}. Samples were solubilized at 2.5 mg mL^{-1}, stirred overnight, and filtered through a 0.45 μm nylon filter prior to injection. UV detection (λ = 260 nm) was used to obtain the spectra. Relative molar masses were determined using sodium polystyrene sulfonates (PSS) with molar masses ranging from 891 to 258 000 g mol^{-1} as standards.

Particle sizes, morphologies and surface charge

The solutions were prepared at a concentration of 1 g L^{-1}.

Dynamic light scattering (DLS) and zeta potential analyses were carried out using a Zetasizer Nano ZS (Malvern) operating with a He–Ne laser source (λ = 633 nm, scattering angle = 173°). Each sample was analyzed in triplicates at room temperature.

Transmission electron microscopy (TEM) analyses were performed using a HITACHI H7650 apparatus operating at 80 kV. About 10 μL of the samples were deposited on 150 mesh copper grids, covered with a carbon film and hydrophilized using a plasmacleaner (Fischione Model 1070 nanoclean) and the excess was removed after 1 minute. The images were captured with an 11 MPix ORIUS (Gatan) CCD camera.

Surface and interfacial tensions

Surface and interfacial tensions were measured using a DSA100 drop shape analyzer (KRÜSS). The measurements were conducted at room temperature using the pendant drop method with the Laplace model. For surface tension measurements, aqueous drops with varying lignin concentrations were formed in air, and at least three measurements were taken for each sample. For interfacial tension measurements, aqueous solutions with 2 wt% lignin were used to form drops in sunflower oil. The drops were progressively formed and were given 2 minutes to stabilize before measurements were conducted.

Emulsions preparation

Emulsions were prepared following a protocol aiming at obtaining oil-in-water (O/W) emulsion with the concentration being 20 : 80 w/w. Mixtures of lignin in water (2.5 wt%) were placed under Ultra-turrax shearing (T 25 digital, IKA). The speed was set to 8000 rpm, and the adequate volume of sunflower oil was added dropwise. The shearing was maintained for 5 minutes. The nature of the emulsion (O/W or W/O) was confirmed by a drop test consisting in adding a drop of the emulsion to a small volume of either water or oil phase. The continuous phase was identified as the one in which the drop was well diluted. The formed emulsions were stored at room temperature.

Emulsions characterization

Emulsion characterization analyses were performed no more than a few hours after emulsification.

For optical microscopy, a drop of the emulsion was placed on a cavity slide, covered with a cover slip, and observed using a Zeiss AxioStar microscope equipped with a ×10 objective (CP-Achromat, Zeiss) and a digital camera (Axiocam 208 color, Zeiss).

Laser diffraction granulometry was conducted using a Mastersizer 3000 laser diffraction device (Malvern) to deter-

mine the size distributions of the emulsion droplets, based on Mie theory. The analyses were performed at room temperature by dispersing emulsion droplets in a chamber containing deionized water.

Emulsion stability was assessed by measuring separation, using a LUMiFuge apparatus (LUM GmbH) involving the Space and Time Resolved Extinction Profiles (STEP) technology. Samples were placed into analysis tubes and centrifuged at 800*g* for 30 minutes at 25 °C to accelerate destabilization. The transmittance of the samples was monitored all along the tube throughout centrifugation using a near-infrared light (λ = 865 nm) emission and detection system. Each light impulsion provided a transmittance profile reflecting destabilization phenomena. The separation indexes were determined from each extinction profile and allowed to plot the evolution of the separation index as a function of time. The analysis was carried out in duplicates for each emulsion.

Results and discussion

Like most lignins obtained from alkaline pretreatment, the alkali lignin (AL) used in this study is insoluble in both acidic and neutral water. Our first achievement was the solubilization of this lignin in water at pH values as low as 2. This was accomplished thanks to a two-step protocol involving water and acetone as shown on Fig. 1.

In a first step, the use of a 50 : 50 mixture of both solvents allowed the dissolution of 98.4 wt% of AL, based on the mass yield of the insoluble part. These results could be correlated with the Hansen solubility parameters (δ_d, δ_p, δ_h) of the different substances. The parameters δ_p and δ_h quantify the polar and hydrogen bonding interactions, respectively. Mixing water and acetone yields a decrease of δ_p and δ_h by diminishing the polarity and hydrogen bonding ability in comparison to pure water (Table 1). The resulting δ_p and δ_h values (13.2 and 24.7 $MPa^{1/2}$ respectively) tend to be similar to those of solvents known to solubilize lignin such as dimethylformamide (DMF) or dimethyl sulfoxide (DMSO).[36] In such mixture, polar interactions and hydrogen bonding between lignin and the solvent were thus enhanced. Moreover, water is known to act as a plasticizer, allowing solvent diffusion within lignin aggregates due to its small molecular size.[37,38] This first step was repeated six times and demonstrated high reproducibility for different mass scales (initial AL mass ranging from 5 g to 20 g) and batches of alkali lignin. In most attempts, the starting lignin concentration was set to 10 wt%, but it was proved the experience can be conducted up to a 15 wt% lignin concentration.

Table 1 Hansen solubility parameters of some usual solvents or mixture of solvents

Solvent	δ_d ($MPa^{1/2}$)	δ_p ($MPa^{1/2}$)	δ_h ($MPa^{1/2}$)
Water	15.5	16.0	42.3
Acetone	15.5	10.5	7.0
Water/acetone (50 : 50)	15.5	13.2	24.7
DMF	17.4	13.7	11.3
DMSO	18.4	16.4	10.2

In the second step, the acetone was removed by evaporation under reduced pressure, and the adequate volume of water was added to the solution to maintain the initial concentration. Despite its initial insolubility, the lignin did not precipitate under these conditions and the mixture looked stable in appearance. After stirring, a major part of the lignin (94.7 wt%) was still soluble (Fig. 2), and the protocol was once again reproducible (Fig. 1). Overall, this two-step process allowed the solubilization in water of more than 93 wt% of the initial quantity of AL. The pH of the solution of lignin in water was acidic (pH = 3.5) (Table 2), value attributed to the presence of carboxylic acids (pK_a around 4) on the lignin structure.[39] Following this, a small fraction of the lignin solution was intentionally freeze-dried to evaluate the lignin molecular structure.

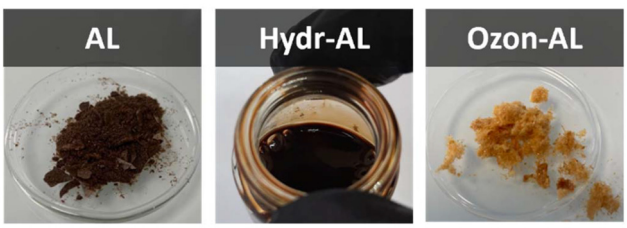

Fig. 2 Visual aspect of alkali lignin (AL), water solubilized lignin (Hydr-AL) and ozonated lignin (Ozon-AL) (discussed below).

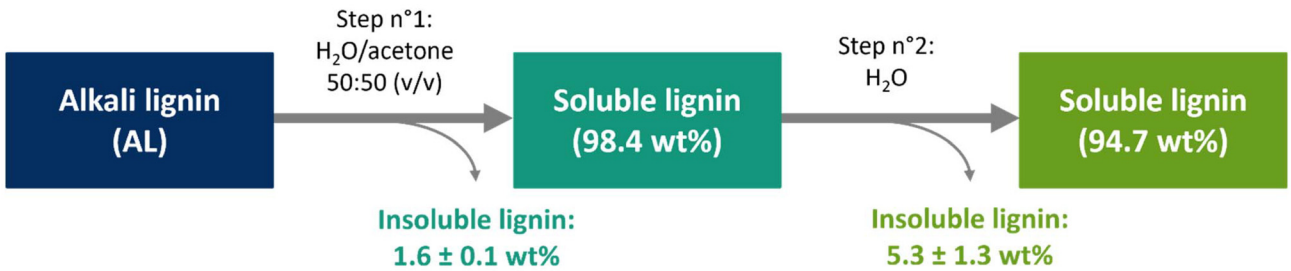

Fig. 1 Schematic representation of the 2-step solubilization process.

Table 2 OH quantification by ^{31}P NMR, mass yields and pHs of the aqueous solutions for AL, Hydr-AL (after drying) and Ozon-AL (discussed below)

	OH groups quantification (mmol g^{-1})						
	Aliph-OH	Ph-OH	CO-OH	Mass yield	pH	M_w (g mol^{-1})	$Đ$
AL	1.62	2.51	0.48	—	—	18 500	7.7
Hydr-AL	1.62 ± 0.08	2.54 ± 0.09	0.42 ± 0.02	—	3.5 ± 0.0	18 800	9.8
Ozon-AL	0.98 ± 0.05	0.18 ± 0.02	1.23 ± 0.19	105.0 ± 8.5%	2.7 ± 0.2	4100	3.6

Quantitative ^{31}P NMR (Table 2 and Fig. S2†) and SEC analyses (Fig. 3 and Table 2) did not show any significant change in the hydroxyl functions content and molar masses between AL and the water-solubilized lignin, referred as Hydr-AL. These results indicated that no chemical modifications or depolymerization/condensation reactions occurred during the process, and that Hydr-AL remained largely unchanged compared to AL. It was also shown, after freeze-drying, that Hydr-AL could not be solubilized in water anymore. We hypothesized that, during the drying step, Hydr-AL forms aggregates through strong intramolecular hydrogen bonds,[40] reducing the number of sites available for water interaction and consequently hindering its resolubilization in water. However, by reintroducing dried Hydr-AL into a 50 : 50 (v/v) water/acetone mixture and subsequently evaporating the acetone, Hydr-AL could be fully resolubilized in water once again, demonstrating the crucial role of the solvent mixture.

In a second stage, the lignin was chemically modified through reactions compatible with water as a solvent, to enhance its hydrophilicity. Oxidation reactions are well-suited for this purpose,[41] and, based on previous work, ozonation was selected.[42] The ozonation conditions were optimized and details are provided in the ESI (Table S1 and Fig. S3†). The optimized ozonation reaction was conducted on a diluted solution of Hydr-AL to minimize foaming, with ozone generated by a *corona* discharge ozone generator and bubbled into the solution for 10 minutes at room temperature. Ozone was applied to the water dispersion rather than the water/acetone mixture because acetone would evaporate during the process, making its presence useless while also altering the lignin concentration in an uncontrolled manner. In each case, mass yields slightly exceeded 100%, suggesting the absence of material loss and the likely incorporation of oxygen into the lignin.

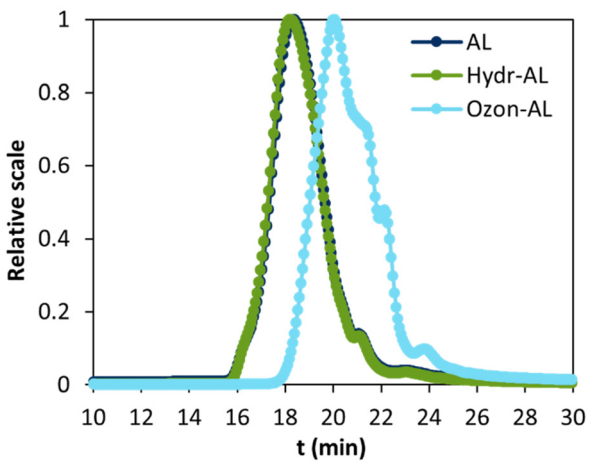

Fig. 3 Molar masses distribution for AL, Hydr-AL (after drying) and Ozon-AL (discussed below).

The product was also submitted to ^{31}P NMR (Fig. S2†) and hydroxyls quantification is available in Table 2 where the oxidized lignin is referred as Ozon-AL. After ozonation, the amount of carboxylic acids increased notably (+193%), while the phenolic hydroxyl groups showed a significant drop (−93%). As shown by the mechanism illustrated in Scheme 1a (see Scheme S1† for detailed mechanism), the oxidation reaction leads to the cleavage of aromatic rings resulting in the formation of muconic acid-derived carboxylic acids and esters under acidic conditions.[43,44] The pH of the aqueous solution of ozonated lignin showed a slight decrease (pH = 2.7 ± 0.2) (Table 2) supporting the formation of new carboxylic acid functions. Furthermore, the cleavage of aromatic rings, that are some of the lignin chromophore groups, was also confirmed by the brightening of the samples after ozonation (Fig. 2).

SEC analysis (Fig. 3 and Table 2) showed a significant decrease in molar masses and dispersity, likely due to the breakdown of aromatic structures and possibly to the disruption of structures such as stilbenes.[45]

FT-IR spectra (Fig. 4) of the product before and after ozonation revealed the diminution of the signals at 1510, 1455, 1420 and 1590 cm^{-1} corresponding to C=C aromatic stretching and the overall intensification of the signals between 1800 and 1615 cm^{-1} corresponding to the stretching of conjugated and non-conjugated C=O. The appearance of new carboxylic acids/esters could be confirmed by the intensification of the 1715 cm^{-1} signal while the 1630 cm^{-1} signal suggested the formation of conjugated ketones from α-hydroxyl groups oxidation, for instance.[46] The latter could account for the decrease in aliphatic hydroxyl content determined by ^{31}P NMR analysis (Table 2). The zone between 1650 and 1700 cm^{-1} could in part correspond to the formation of quinone structures. This would probably result from the oxidation of phenols, as described in Scheme 1b (see Scheme S1† for detailed mechanism), and explain why the increase in carboxylic acids does not fully compensate the decrease in phenols as observed in the OH quantification.[47]

Finally, Fig. 5 shows the HSQC spectra of lignin before and after ozonation. A closer view of the aromatic region (Fig. 5, right) confirmed the disruption of phenol moieties, as

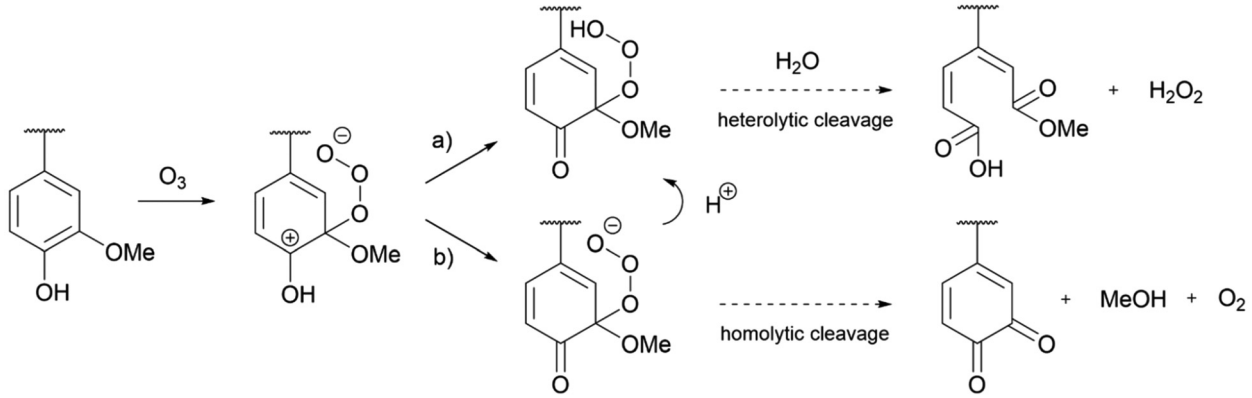

Scheme 1 Proposed mechanism for the effect of ozone on lignin phenol groups through (a) heterolytic cleavage (acidic conditions) and (b) homolytic cleavage.

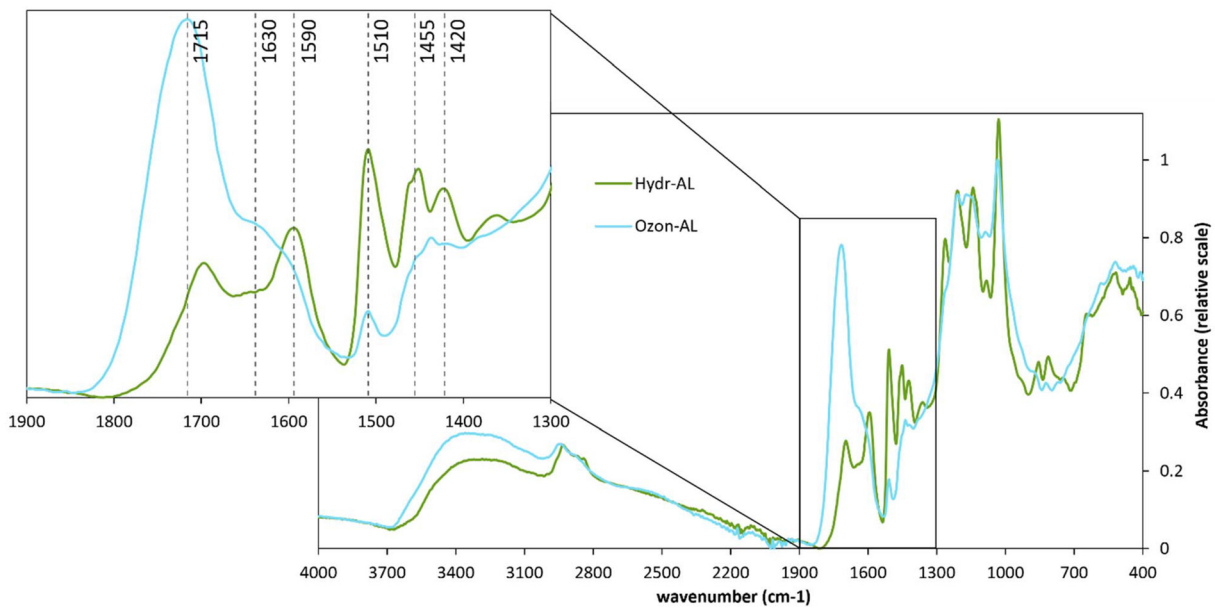

Fig. 4 FT-IR spectra of Hydr-AL (after drying) and of Ozon-AL.

observed in ^{31}P NMR and FT-IR spectroscopy. This is further supported by the loss of aromatic methoxy groups, as evidenced around 3.2–4.3/55.0–57.6 (δ_H/δ_C) ppm (Fig. 5, left). The ozonated lignin also displayed a new signal around 3.5–3.9/51.0–53.2 (δ_H/δ_C) ppm, which corresponds to esters or acetals according to data from literature,[48] and probably confirming the formation of methyl esters as described by Scheme 1a. The HSQC analysis also revealed the apparent cleavage of some lignin characteristic bonds, such as residual β-O-4′ or β–β′ in the case of AL (Fig. 5, left), results that were not identified through the previous characterization techniques, but could explain the molar masses decrease.

Nevertheless, this oxidation process resulted in a lignin with enhanced hydrophilicity, as solubility tests performed on freeze-dried Ozon-AL showed that only 15.0 ± 2.8% of it was insoluble in water, unlike freeze-dried Hydr-AL. This result was attributed to aromatic structures cleavage and the increased amounts of hydrophilic oxygenated functions such as carboxylic acids and ketones leading to higher water solubility. The reaction was performed four times with good reproducibility.

Then, the Hydr-AL solution was diluted without pH adjustment (pH = 3.5), while dried Ozon-AL was resolubilized in water, yielding an acidic aqueous solution (pH = 2.7). Both preparations, at a concentration of 1 g L^{-1}, were used for DLS, zeta potential, and TEM analyses, which highlighted key features.

DLS results (Fig. 6a and Table S2†) and TEM images (Fig. 7) revealed the presence of nano-sized objects within the lignin samples in water. Thus, although these "solutions" appear homogeneous, they can more accurately be described as nanodispersions. Solubilization refers to the formation of a homo-

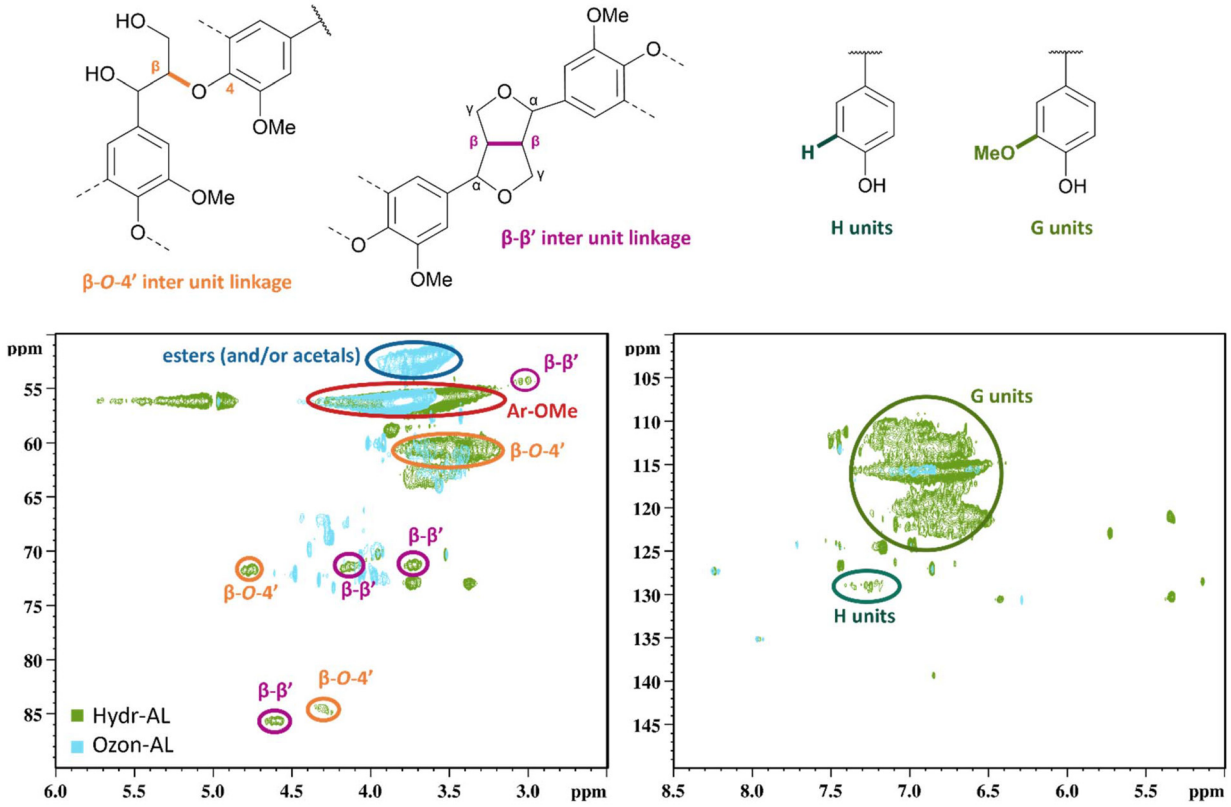

Fig. 5 2D HSQC NMR spectra of selected area (left: aliphatic region, right: aromatic region) of Hydr-AL (after drying) and Ozon-AL.

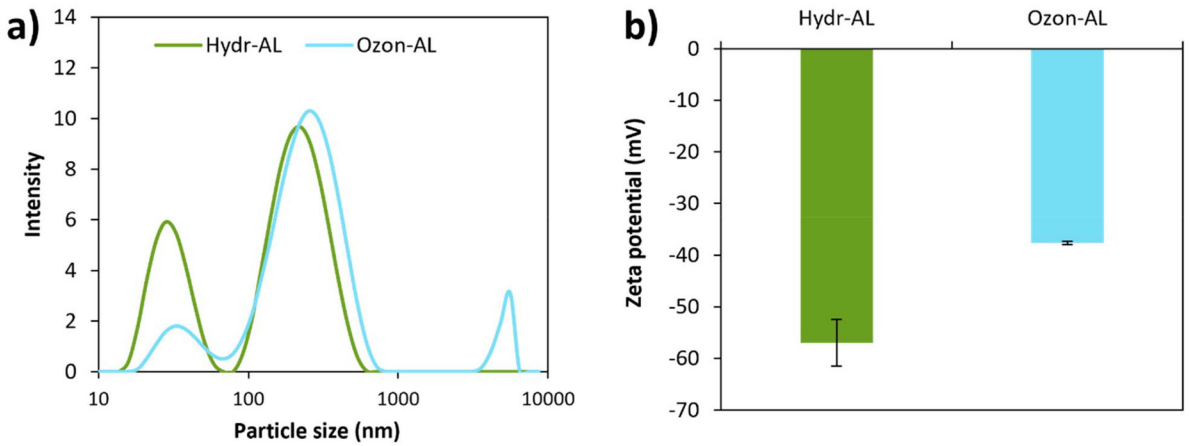

Fig. 6 (a) Intensity particle size distributions and (b) zeta potential for aqueous solutions, of Hydr-AL and Ozon-AL (c = 1 g L^{-1}).

geneous solution where polymer chains are dispersed at the molecular scale, typically resulting in no detectable aggregates by DLS, while dispersion, in this case, is defined by the presence of particles ranging from tens to hundreds of nm, as confirmed by both DLS and TEM analyses. In parallel, zeta potential measurements (Fig. 6b and Table S2†) indicated that these nano-objects carry a negative surface charge. The stability of such dispersions is due to the small size and high surface charge (absolute value) of the nano-objects, preventing their sedimentation. The particle size distributions were multimodal for both dispersions. In the case of Hydr-AL, the dispersion consisted of a few large quasi-spherical particles measuring approximately 230 nm and a majority of irregularly shaped objects measuring around 30 nm (Fig. 6a and 7a–c). These nano-objects likely resulted from the previous two-step "solubilization" process involving acetone and water, which is similar to anti-solvent precipitation methods often used to form lignin nanoparticles (LNPs). This process typically con-

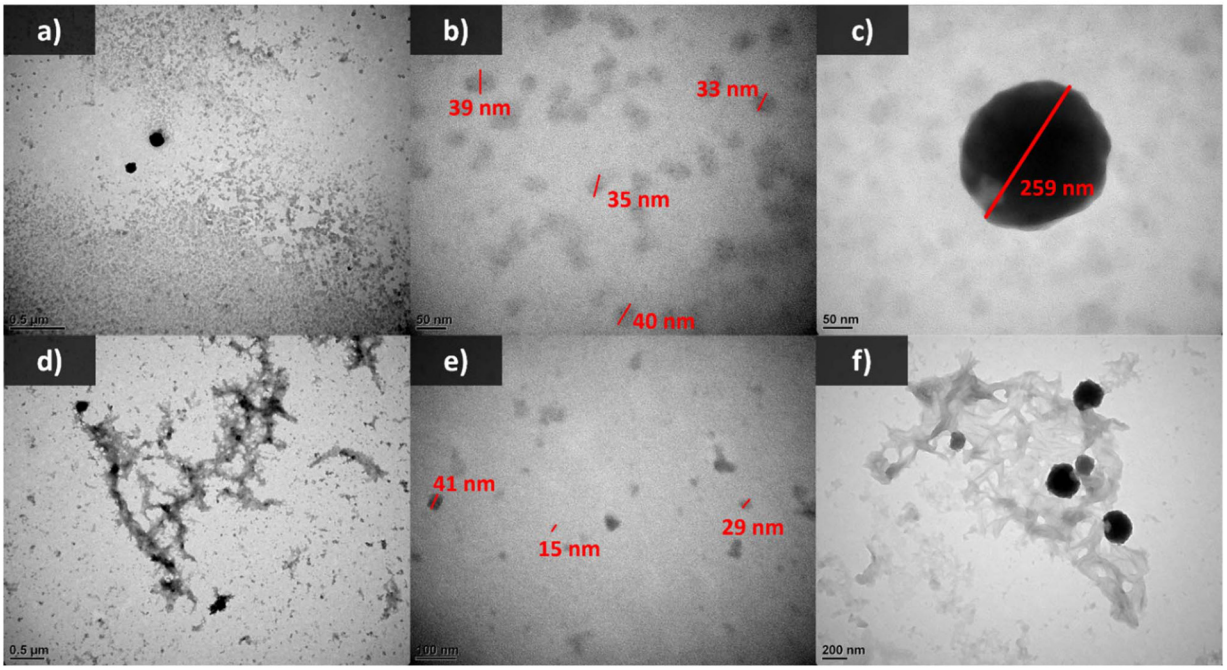

Fig. 7 TEM images of the aqueous solutions of (a–c) Hydr-AL (d–f) Ozon-AL (c = 1 g L^{-1}).

sists of an initial solubilization step in a good solvent (water/acetone mixture) followed by precipitation in an anti-solvent (pure water).[36,49] In the present work, the particle size distribution is quite broad, and the particle morphologies are not completely spherical, indicating poor control over LNP formation, which was not the initial objective of the protocol. In the case of Ozon-AL, the particles exhibited larger heterogeneity in both size and morphology. DLS and TEM results (Fig. 6a and 7d–f) revealed, once again, the presence of nano-objects measuring a few dozen nanometers, as well as particles around 200 nm in size, both displaying less defined shapes compared to those observed previously. Additionally, unshaped aggregates with size exceeding a micrometer could be observed. The chemical effects of ozonation resulted in two distinct behaviors: the formation of micrometer-sized aggregates, which likely represent the lignin fraction that sediments (15%) and was previously considered "insoluble", and the stabilization of smaller particles (less than 200 nm) in dispersion. As described in the literature,[50] micrometer-sized aggregates may form due to the modification of lignin during ozonation, which alters particle interactions and leads to colloidal destabilization. Additionally, such aggregation may also result from the freeze-drying process of Ozon-AL after ozonation, followed by re-dispersion in water. This could explain the relatively low zeta potential (absolute value) observed for Ozon-AL compared to Hydr-AL, due to charge screening, despite the higher carboxyl group content. On the other hand, the increased hydrophilic functions likely enhanced lignin interaction with water, preventing aggregation through formation of stable smaller particles. A higher content of carboxylic acid groups also suggests stronger electrostatic repulsions, thereby improving stabilization. In fact, the lower zeta potential (absolute value) observed after ozonation may not accurately reflect the true surface charge of the smallest particles, as the presence of larger aggregates could bias the measurement. Furthermore, the degradation of aromatic structures could have resulted in the formation of smaller, more dispersed particles.[50]

Regardless of such behavior, Hydr-AL and Ozon-AL were then evaluated in terms of surface activity.

Lignin behavior at water/air and water/oil interfaces and emulsion stabilization

Using the pendant drop method in air, we demonstrated that both Hydr-AL and Ozon-AL reduced the surface tension of water (Fig. 8), confirming their ability to adsorb at the water/air interface and thus their interfacial activity. This effect was mainly attributed to the adsorption of the smallest particles (30 nm), which are probably faster at reaching the interface. The surface tension decreased as the lignin concentration increased due to the adsorption of more particles at the water/air interface. Interestingly, no break in the slope of the curves was observed, suggesting the absence of a critical aggregation concentration (CAC), which is likely inherent to the morphology of the nano-objects. Ozon-AL appeared to adsorb at the interface more efficiently than Hydr-AL, achieving surface tensions as low as 48 mN m^{-1}, compared to 51 mN m^{-1} at higher concentrations for Hydr-AL. These values are consistent with those commonly reported in the literature.[14] The difference between both lignins could be attributed to the chemical modifications in Ozon-AL, where the cleavage of aromatic structures and the enrichment in carboxylic acid groups

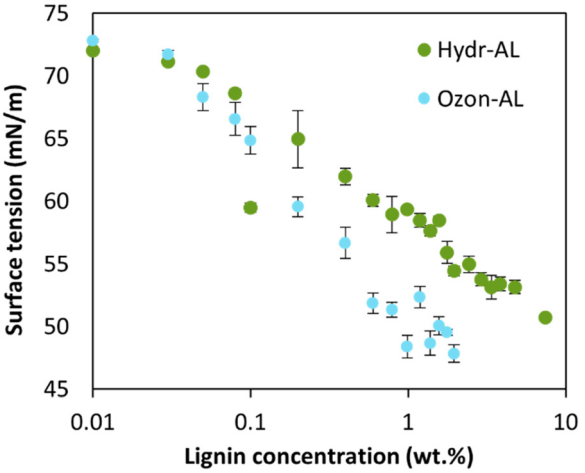

Fig. 8 Surface tensions for aqueous solutions of Hydr-AL and Ozon-AL as a function of the lignin concentration.

provide chain flexibility and, above all, enhance interfacial affinity compared to Hydr-AL. Moreover, the presence of micro-sized aggregates within Ozon-AL may have hindered its adsorption at the interface by reducing the effective amount of dispersed lignin available and limiting the diffusion of individual lignin particles, potentially leading to an underestimation of its ability to reduce surface tension.

Interfacial tensions (Table 3) were measured between water and sunflower oil using 2 wt% lignin solutions which revealed trends similar to those observed for surface tensions as reported in the literature.[21,31] Both lignins seemed able to decrease the interfacial tension of a water/sunflower oil system by positioning themselves at the oil/water interface. These results further confirmed the amphiphilic nature of the lignins. Ozon-AL was particularly effective at reducing interfacial tension, likely due to its stronger affinity for the oil phase, as previously discussed.

Both surface and interfacial tension measurements demonstrated Hydr-AL and Ozon-AL ability to adsorb at the interfaces. The reduction in oil/water interfacial tension indicated promising emulsion stabilization properties, especially for Ozon-AL. Subsequently, the lignin dispersions were involved in the formulation of emulsions with 20 wt% sunflower oil. A lignosulfonate (LS) was used as a reference, and the corresponding emulsion was prepared without pH adjustment, resulting in a pH of 7. Oil-in-water (O/W) emulsions were successfully obtained suggesting the effective adsorption of lignin particles at the surface of the oil droplets (Fig. 9). All emulsions exhibited rapid creaming (not visible in the images), which typically occurs due to the upward movement of droplets larger than 1 μm. Despite this, no oil release or sedimentation were observed in short times (a few minutes).

Table 3 Interfacial tensions for aqueous solutions of Hydr-AL and Ozon-AL (c = 2 wt%)

	Water/sunflower oil interfacial tension (mN m^{-1})
None	20–28[51,52]
Hydr-AL	13.7 ± 0.8
Ozon-AL	7.8 ± 1.7

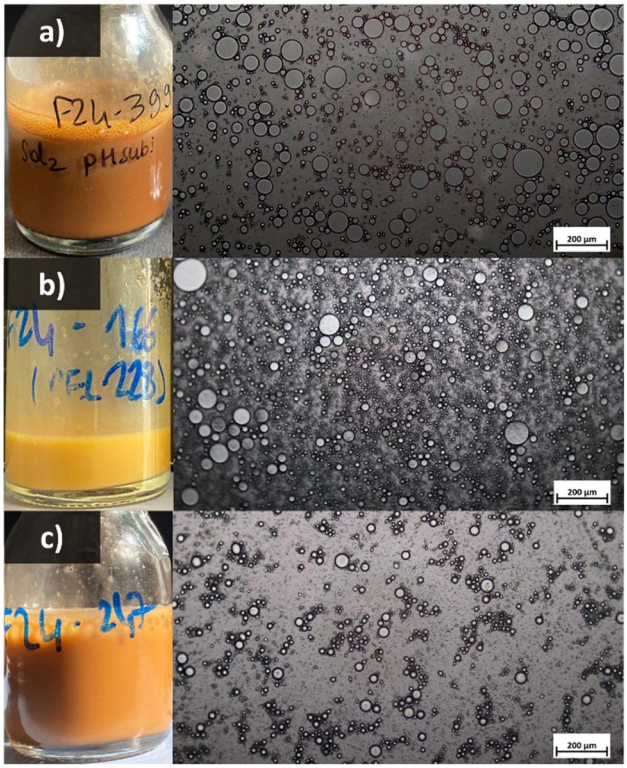

Fig. 9 Visual aspect and optical microscopy image (×10 objective lens, scale bar indicates 200 nm) of O/W (20 : 80 w/w) emulsions prepared from aqueous solutions of (a) Hydr-AL, (b) Ozon-AL, and (c) LS, with the lignin representing 2 wt% of the total emulsion in each case.

Each emulsion was homogenized and examined using optical microscopy (Fig. 9). In all cases, the droplet sizes were polydisperse, likely due to the relatively low shear rate (8000 rpm) used during preparation. Some flocculation was also visible in all systems, but particularly for the emulsion obtained from lignosulfonate (LS), which could indicate a lack of electrostatic repulsions despite a higher pH value, generally associated with higher ionization degree due to carboxylic acid deprotonation. Granulometry analyses were conducted under diluted conditions, on the assumption that the oil droplets were likely de-flocculated, although this was not explicitly confirmed. Additionally, it should be noted that lignin particles are also detected by granulometry, and that their presence likely influences the measurement outcomes. Nonetheless, the droplet size distribution (Fig. 10 and Table S3†) confirmed the polydispersity of the systems. Minor differences in size were observed between Hydr-AL and LS-based emulsions ($D_{4,3}$ around 30 μm) while Ozon-AL-based emulsion exhibited a slightly larger droplet mean size ($D_{4,3}$ around 50 μm). Such values are consistent with literature data where sizes generally range from 10 to 100 μm.[21]

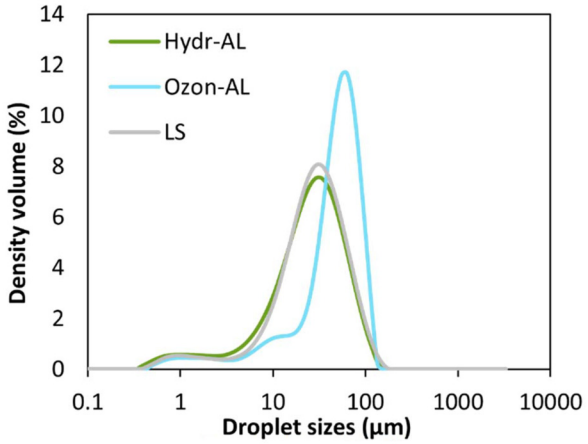

Fig. 10 Droplet sizes distribution of O/W (20 : 80 w/w) emulsions prepared from aqueous solutions of Hydr-AL, Ozon-AL and LS.

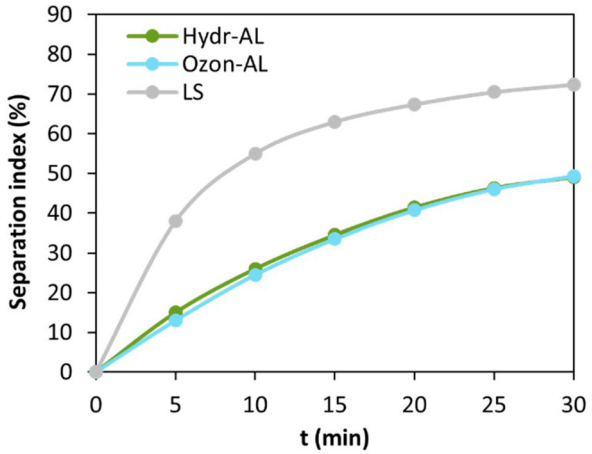

Fig. 12 Separation indexes obtained for O/W (20 : 80 w/w) emulsions prepared from aqueous solutions of Hydr-AL, Ozon-AL and LS, as a function of centrifugation time.

To further discriminate the different systems, the stability of the emulsions was evaluated by means of analytical centrifugation (800*g*, 30 min, 25 °C). Analytical centrifugation allows the monitoring of gravity-dependent destabilization mechanisms such as creaming, sedimentation, or oil release in an accelerated way. Separation indexes reflect the degree of oil and water phases separation and can be plotted against centrifugation time. Once again, Hydr-AL and Ozon-Al were compared to LS: their appearance after centrifugation and separation indexes are presented in Fig. 11 and 12 and the transmittance profiles are presented in Fig. S4.†

Emulsions prepared from Hydr-AL and Ozon-AL did not show oil release even after centrifugation (Fig. 11a and b) while the emulsion prepared from LS released oil during centrifugation (Fig. 11c) indicating insufficient stabilizing ability. None of the emulsions exhibited sedimentation, indicating that the separation indexes reflect only the behavior of the oil droplets. In all cases, creaming occurred progressively (Fig. 12 and Fig. S4†), which is consistent with droplet polydispersity, as the largest droplets rose first, followed by smaller ones. The separation index values demonstrated that emulsions prepared with Hydr-AL and Ozon-AL exhibited similar stabilizing abilities and were quantitatively more stable than the LS emulsion, with separation indexes below 50% compared to over 72% for LS at the end of centrifugation. Furthermore, the emulsions prepared from Hydr-AL exhibited only small oil droplets at the surface, while the Ozon-AL emulsion showed no visible changes over a 30-day stability assessment at room temperature. In contrast, the LS emulsion released oil over the same period of time. These results demonstrate the effectiveness of the prepared lignins in stabilizing O/W emulsions. The stabilization mechanism of lignin is known to involve a combination of electrostatic and steric effects, which depends on factors such as lignin structure, amphiphilicity, surface charge, or packing behavior.[53] On one hand, the low stabilizing ability of LS was attributed to an irreversible destabilization mechanism such as coalescence or Ostwald ripening. The latter phenomenon was not considered as it involves the partial solubility of the dispersed phase in the continuous one, and sunflower oil is insoluble in water. Therefore, the low stabilization was attributed to coalescence driven by flocculation. Coalescence could also result from the insufficient affinity of LS for the oil phase, resulting in insufficient coverage of the oil droplets.

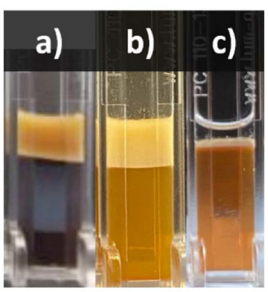

Fig. 11 Visual aspect of O/W (20 : 80 w/w) emulsions prepared from aqueous solutions of (a) Hydr-AL, (b) Ozon-AL, and (c) LS, after analytical centrifugation (800*g*, 30 min, 25 °C).

On the other hand, we assumed a different stabilization mechanism concerning Hydr-AL and Ozon-AL. The centrifugation process demonstrated that polydispersity and flocculation did not necessarily compromise the Hydr-AL and Ozon-AL emulsions stability, as reported in the literature.[29] We hypothesized the emulsion stabilization was mainly due to 30 nm-sized particles, as they were more numerous, thus acting as Pickering particles. Such particles are characterized by their high adsorption energy at the oil–water interfaces, which could explain the superior stability observed in these systems.[16] Additionally, stabilization might partly result from the adsorption of a soluble fraction of lignin, though its proportion remains unknown. Such mechanism is described as synergistic stabilization in previous studies and relies on a

delicate balance in lignin aggregation: excessive aggregation can prevent efficient adsorption at the droplet surface.[31] Here, despite low pH conditions, the systems did not lead to excessive lignins aggregation, maintaining their stabilizing function. Nonetheless, it has to be noted that Ozon-AL and Hydr-AL displayed similar stabilizing performance while Ozon-AL was more efficient at reducing surface and interfacial tensions. This could be explained by the higher heterogeneity in particle sizes and morphologies in Ozon-AL, as well as the presence of large aggregates, as previously discussed.[31,49] Addressing this issue remains a key challenge. However, Ozon-AL demonstrated slightly better long-term stability, further highlighting the potential of ozonation to enhance the surface activity of lignin.

Finally, an emulsion test using an Ozon-AL solution at pH 12 (Fig. S5†) demonstrated very poor affinity for the oil phase and low stabilization ability. This likely resulted from the strong hydrophilicity of lignin at such pH. These findings are promising for developing pH-sensitive systems for diverse applications.[54]

Conclusion

A simple two-step process using benign solvents (water and acetone) enabled the stable dispersion of alkali lignin in water under acidic conditions. This stability was achieved through the combined interactions of both solvents with lignin. The resulting aqueous dispersion contained bimodal-sized particles that effectively reduced the surface tension of water and the interfacial tension in a water/oil system. Furthermore, it demonstrated strong O/W emulsion stabilization with just 2 wt% of surface-active agents, mainly attributed to the adsorption of 30 nm-sized Pickering particles at the oil droplet surface. The affinity of this lignin for the interface could be enhanced through an oxidation step. The aqueous dispersion could undergo ozonation which mainly yielded a carboxylic acid-enriched lignin, due to the cleavage of aromatic structures. The conditions were optimized to design a short and straightforward process requiring only water and no harmful chemicals, complex protocol, purification or need for alkalinization, as often described in the literature. A key next step would be to investigate the scalability of the ozonation process at an industrial level, considering both reaction parameters (lignin concentration, reaction time, temperature, gas flow rate, electric field power, ozone release method, *etc.*) and the degradation of residual ozone, given its potential toxicity in the lower atmosphere. Nevertheless, the ozonated lignin could be easily re-dispersed in water, which led to an acidic dispersion characterized by stable bimodal nanoparticles. These nanoparticles displayed an even stronger affinity for both water/air and water/oil interfaces, leading to the successful stabilization of oil-in-water Pickering emulsions for at least 30 days. Overall, this study demonstrated the potential of a straightforward, reproducible and environmentally friendly route to modify an industrial alkali lignin, as an effective surface agent for emulsion stabilization. Expanding these protocols to lignins of different origins and assessing the properties of the resulting products would further demonstrate the versatility and broad applicability of the dispersion and ozonation processes.

Data availability

The data supporting this article have been included as part of the ESI.†

Conflicts of interest

The authors declare no competing financial interest.

Acknowledgements

The authors gratefully acknowledge the financial support from Région Nouvelle Aquitaine and ITERG (French institute for fats and oils).

References

1 N. Dahmen, I. Lewandowski, S. Zibek and A. Weidtmann, *GCB Bioenergy*, 2019, **11**, 107.
2 F. G. Calvo-Flores, J. A. Dobado, J. Isac-García and F. J. Martín-Martínez, in *Lignin and Lignans as Renewable Raw Materials*, ed. F. G. Calvo-Flores, J. A. Dobado, J. Isac-García and F. J. Martín-Martínez, John Wiley & Sons, Hoboken, 2015, ch. 4, pp. 75–112.
3 F. G. Calvo-Flores, J. A. Dobado, J. Isac-García and F. J. Martín-Martínez, in *Lignin and Lignans as Renewable Raw Materials*, ed. F. G. Calvo-Flores, J. A. Dobado, J. Isac-García and F. J. Martín-Martínez, John Wiley & Sons, Hoboken, 2015, ch. 3, pp. 49–74.
4 R. Vanholme, B. Demedts, K. Morreel, J. Ralph and W. Boerjan, *Plant Physiol.*, 2010, **153**, 895.
5 J. Lora, in *Monomers, Polymers and Composites from Renewable Resources*, ed. M. N. Belgacem and A. Gandini, Elsevier, Amsterdam, 2008, ch. 10, pp. 225–241.
6 D. Kai, M. J. Tan, P. L. Chen, Y. K. Chua, Y. L. Yap and X. J. Loh, *Green Chem.*, 2016, **18**, 1175.
7 T. Aro and P. Fatehi, *ChemSusChem*, 2017, **10**, 1861.
8 N. Alwadani and P. Fatehi, *Carbon Resour. Convers.*, 2018, **1**, 126.
9 K. M. Askvik, S. Are Gundersen, J. Sjöblom, J. Merta and P. Stenius, *Colloids Surf., A*, 1999, **159**, 89.
10 C. Shi, S. Zhang, W. Wang, R. J. Linhardt and A. J. Ragauskas, *ACS Sustainable Chem. Eng.*, 2020, **8**, 22.
11 K. M. Perkins, C. Gupta, E. N. Charleson and N. R. Washburn, *Colloids Surf., A*, 2017, **530**, 200.
12 B. V. K. J. Schmidt, V. Molinari, D. Esposito, K. Tauer and M. Antonietti, *Polymer*, 2017, **112**, 418.

13 C. Gupta and N. R. Washburn, *Langmuir*, 2014, **30**, 9303.
14 S. Li, J. A. Willoughby and O. J. Rojas, *ChemSusChem*, 2016, **9**, 2460.
15 S. Li, D. Ogunkoya, T. Fang, J. Willoughby and O. J. Rojas, *J. Colloid Interface Sci.*, 2016, **482**, 27.
16 N. Ghavidel and P. Fatehi, *Langmuir*, 2021, **37**, 3346.
17 K. Chen, S. Yuan, D. Wang, Y. Liu, F. Chen and D. Qi, *Langmuir*, 2021, **37**, 12179.
18 A. Yuliestyan, P. Partal, F. Navarro, R. Martín-Sampedro, D. Ibarra and M. E. Eugenio, *Polymers*, 2022, **14**, 2879.
19 G. Shulga, V. Shakels, S. Skudra and V. Bogdanovs, *Environ. Technol. Resour. Proc. Int. Sci. Pract. Conf.*, 2011, **1**, 276.
20 J. Ruwoldt, R. Skunde, M. Tanase-Opedal and K. Syverud, *Ind. Crops Prod.*, 2025, **223**, 120019.
21 S. Gharehkhani, N. Ghavidel and P. Fatehi, *ACS Sustainable Chem. Eng.*, 2019, **7**, 2370.
22 S. Chen, H. Liu, H. Sun, X. Yan, G. Wang, Y. Zhou and J. Zhang, *J. Mol. Liq.*, 2018, **249**, 73.
23 S. Chen, X. Zhou, J. Yang, Y. Dai, W. Wang, W. Jiang, X. Li and J. Zhang, *J. Mol. Liq.*, 2023, **390**, 123072.
24 B. Košíková, M. Ďuriš and V. Demianová, *Eur. Polym. J.*, 2000, **36**, 1209.
25 Z. Zhang, Y. Zhang, Z. Lin, A. Mulyadi, W. Mu and Y. Deng, *Chem. Eng. Sci.*, 2017, **165**, 55.
26 J. Ruwoldt, B. Handiso, M. Øksnes Dalheim, A. Solberg, S. Simon and K. Syverud, *Langmuir*, 2024, **40**, 5409.
27 J. Zhang, Y. Ge, L. Qin, W. Huang and Z. Li, *J. Dispersion Sci. Technol.*, 2018, **39**, 1140.
28 Q. Xu, Y. Bai, X. Zhao, M. Ren, S. Wang and F. Kong, *Ind. Crops Prod.*, 2021, **164**, 113376.
29 R. Álvarez-Barajas, A. A. Cuadri, F. J. Navarro, F. J. Martínez-Boza and P. Partal, *Polymers*, 2021, **13**, 2703.
30 A. Czaikoski, A. Gomes, K. C. Kaufmann, R. B. Liszbinski, M. B. de Jesus and R. L. Cunha, *Ind. Crops Prod.*, 2020, **154**, 112762.
31 C. Hadjiefstathiou, A. Manière, J. Attia, F. Pion, P. H. Ducrot, E. Gore and M. Grisel, *J. Mol. Liq.*, 2023, **390**, 123030.
32 S. Bertella, M. Bernardes Figueirêdo, G. De Angelis, M. Mourez, C. Bourmaud, E. Amstad and J. S. Luterbacher, *ChemSusChem*, 2022, **15**, e202200270.
33 P. T. Anastas and J. C. Warner, *Green Chemistry: Theory and Practice*, Oxford University Press, Oxford, 1998.
34 A. Granata and D. S. Argyropoulos, *J. Agric. Food Chem.*, 1995, **43**, 1538.
35 D. S. Zijlstra, A. de Santi, B. Oldenburger, J. de Vries, K. Barta and P. J. Deuss, *J. Visualized Exp.*, 2019, **143**, 1.
36 X. Li, J. Shen, B. Wang, X. Feng, Z. Mao and X. Sui, *ACS Sustainable Chem. Eng.*, 2021, **9**, 5470.
37 J. Wang, Y. Qian, L. Li and X. Qiu, *ChemSusChem*, 2020, **13**, 4420.
38 Y.-Y. Wang, M. Li, C. E. Wyman, C. M. Cai and A. J. Ragauskas, *ACS Sustainable Chem. Eng.*, 2018, **6**, 6064.
39 E. Sjostrom, *Nord. Pulp Pap. Res. J.*, 1989, **4**, 90–93.
40 O. Gordobil, R. Herrera, F. Poohphajai, J. Sandak and A. Sandak, *J. Mater. Res. Technol.*, 2021, **12**, 159.
41 M. Camus, O. Condassamy, F. Ham-Pichavant, C. Michaud, S. Mastroianni, G. Mignani, E. Grau, H. Cramail and S. Grelier, *Polymers*, 2021, **13**, 3725.
42 N. Longhitano, PhD thesis, Université de Bordeaux, 2021.
43 M. B. Figueirêdo, P. J. Deuss, R. H. Venderbosch and H. J. Heeres, *ACS Sustainable Chem. Eng.*, 2019, **7**, 4755.
44 M. Ragnar, T. Eriksson, T. Reitberger and P. Brandt, *Holzforschung*, 1999, **53**, 423.
45 T. Eriksson and J. Gierer, *J. Wood Chem. Technol.*, 1985, **5**, 53.
46 M. V. Bule, A. H. Gao, B. Hiscox and S. Chen, *J. Agric. Food Chem.*, 2013, **61**, 3916.
47 P. Widsten, B. Hortling and K. Poppius-Levlin, *Holzforschung*, 2004, **58**, 363.
48 M. B. Figueirêdo, H. J. Heeres and P. J. Deuss, *Sustainable Energy Fuels*, 2019, **4**, 265.
49 J. Tian, J. Chen, P. Wang, J. Guo, W. Zhu, M. Rizwan Khan, Y. Jin, J. Song and O. J. Rojas, *Green Chem.*, 2023, **25**, 3671.
50 A. E. Alexakis and M. H. Sipponen, *J. Mater. Chem. A*, 2024, **12**, 26772.
51 A. Charisis and E. P. Kalogianni, *Colloids Interfaces*, 2023, **7**, 48.
52 K. Dopierala, A. Javadi, J. Krägel, K.-H. Schano, E. P. Kalogioanni, M. E. Leser and R. Miller, *Colloids Surf., A*, 2011, **382**, 261.
53 L. Bai, L. G. Greca, W. Xiang, J. Lehtonen, S. Huan, R. W. Nugroho, B. L. Tardy and O. J. Rojas, *Langmuir*, 2019, **35**, 571.
54 K. Gao, J. Liu, X. Li, H. Gojzewski, X. Sui and G. J. Vancso, *ACS Sustainable Chem. Eng.*, 2022, **10**, 9334.

